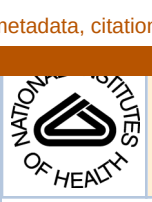

Published in final edited form as:

Bioorg Med Chem Lett. 2011 November 1; 21(21): 6322–6327. doi:10.1016/j.bmcl.2011.08.114.

2-oxo-*N*-aryl-1,2,3,4-tetrahydroquinoline-6-sulfonamides as activators of the tumor cell specific M2 isoform of pyruvate kinase

Martin J. Walsh[a], **Kyle R. Brimacombe**[a], **Henrike Veith**[a], **James M. Bougie**[a], **Thomas Daniel**[a], **William Leister**[a], **Lewis C. Cantley**[b,c], **William J. Israelsen**[d], **Matthew G. Vander Heiden**[d,e], **Min Shen**[a], **Douglas S. Auld**[a,f], **Craig J. Thomas**[a], and **Matthew B. Boxer**[a,*]

[a]NIH Chemical Genomics Center, NIH Center for Translational Therapeutics, National Human Genome Research Institute, National Institutes of Health, 9800 Medical Center Drive, Rockville, Maryland 20850, USA

[b]Division of Signal Transduction, Beth Israel Deaconess Medical Center, Boston, Massachusetts 02115, USA

[c]Department of Systems Biology, Harvard Medical School, Boston, Massachusetts 02115 USA

[d]Koch Institute for Integrative Cancer Research, Massachusetts Institute of Technology, Cambridge, MA 02139, USA

[e]Dana-Farber Cancer Institute, Boston, MA 02115 USA

Abstract

Compared to normal differentiated cells, cancer cells have altered metabolic regulation to support biosynthesis and the expression of the M2 isozyme of pyruvate kinase (PKM2) plays an important role in this anabolic metabolism. While the M1 isoform is a highly active enzyme, the alternatively spliced M2 variant is considerably less active and expressed in tumors. While the exact mechanism by which decreased pyruvate kinase activity contributes to anabolic metabolism remains unclear, it is hypothesized that activation of PKM2 to levels seen with PKM1 may promote a metabolic program that is not conducive to cell proliferation. Here we report the third chemotype in a series of PKM2 activators based on the 2-oxo-*N*-aryl-1,2,3,4-tetrahydroquinoline-6-sulfonamide scaffold. The synthesis, structure activity relationships, selectivity and notable physiochemical properties are described.

Keywords

PKM2; pyruvate kinase; cellular metabolism; anti-cancer strategies; small molecule activators

The M2 isoform of pyruvate kinase (PKM2) is expressed in tumor cells and has been proposed as a diagnostic marker for a large number of cancers[1]. While the expression of this isoform in tumors has been known for a number of years[2], recent work [3–5] has invigorated considerable interest in understanding pyruvate kinase regulation and the possibility of targeting PKM2 for cancer therapy [6–8]. One study has shown that the aberrant metabolism of cancer cells and their production of high levels of lactate in aerobic conditions could be reversed by replacement of the M2 isoform of pyruvate kinase (PK)

Send proofs to: Dr. Matthew B. Boxer, NIH Chemical Genomics Center, NHGRI, National Institutes of Health, 9800 Medical Center Drive, Building B, Room 3005, MSC: 3370, Bethesda, MD 20892-3370, 301-217-4681, 301-217-5736 (fax), boxerm@mail.nih.gov.

[f]Current address: Novartis Institutes for Biomedical Research, Cambridge, Massachusetts 02139, USA.

with the M1 isoform [3]. Rescue of cells subjected to shRNA knock-down of PKM2 with PKM1 also showed reduced tumor formation in a xenograft model. Pyruvate kinase functions in glycolysis to catalyze conversion of phosphoenolpyruvate (PEP) to pyruvate with concomitant generation of ATP from ADP. There are four mammalian PK isoforms encoded by two genes located on two distinct chromosomes [9–13]. Encoded by *PKLR*, PKR is found in erythrocytes and PKL is expressed in both the liver and kidney. The *PKM* gene also has two splice varients; PKM1 that is predominantly found in muscle and brain tissue and PKM2 that is expressed in some adult tissues, embryonic tissues and tumor cells [1]. Regardless of the isoform, the active form of PK is a tetramer. PKM2, PKL and PKR are allosterically activated in a feed forward mechanism by fructose-1,6-bisphosphate (FBP) while PKM1, which is expressed in tissues with high ATP requirements, does not require allosteric activation [14]. While it has been reported that PKM2 in tumors exists predominantly as an inactive dimer [1,15], exactly how this contributes to tumorigenesis and the Warburg effect is still unknown.

It has been hypothesized that cancer cells benefit from the low activity of PKM2 to increase levels of glycolytic intermediates for use in anabolic processes including nucleic acid, amino acid, and lipid syntheses [15]. This suggests that pharmacological activation of PKM2 to levels associated with PKM1 may inhibit cell proliferation as well as be a potential therapeutic strategy for cancer. Our group has previously reported two chemotypes capable of activating PKM2 including a series of diarylsulfonamides [16] and a series of thieno[3,2-b]pyrrole[3,2-d]pyridazinones [17] (exemplified by **1** and **2** respectively in Figure 1). Here, we describe the development of a series of PKM2 activators derived from the 2-oxo-*N*-aryl-tetrahydroquinoline-6-sulfonamide lead, **3**.

Using our previously described qHTS assay for PKM2 activators [16], compound **3** was found to have an AC_{50} = 790 nM in the primary screen. Resynthesis of the hit as well as the majority of analogs described in Tables 1 and 2 was accomplished via base-mediated coupling of commercially available anilines and sulfonyl chlorides in DMF, as represented in Scheme 1. An array of commercially available anilines were coupled with sulfonyl chlorides using either Hunig's base or pyridine in DMF solvent.

We began by looking at potential modification of the aryl linkage, but the importance of the *N*H-sulfonamide was apparent after both the *N*-methylsulfonamide and amide-linked derivatives showed a complete loss in activity (data not shown). We next investigated the importance of the 3,4-dihydroquinolin-2(1H)-one moiety by removing of the amide functionality to generate a number of simple substituted benzene derivates (**5 – 9**). While a number of these retained activity, they all showed significantly diminished potency (≥ 20-fold) and/or efficacy. Informed by these results, we next investigated various amide, urea and carbamate derivatives as well as heteroatom inclusion. A few interesting SAR points from these modifications were: placing the amide carbonyl outside of the ring (**14** and **22)**, changing the amide ring structure to a 5- or 7-membered rings (**15** and **16**) or removing the cyclic nature of the amide (**13** and **17**), all resulted in a significant loss of potency. In general, most analogs that altered the 6-membered lactam moiety saw a considerable drop in activity.

The next SAR we wanted to explore was altering the 3,4-dimethylaniline moiety by addition of a variety of substituted anilines to the commercially available 2-oxo-1,2,3,4-tetrahydroquinoline-6-sulfonyl chloride (Table 2). Preference for substitution of hydrophobic groups at the *meta*-position quickly emerged as a key for potency as the 3-methyl (2**4**), 3-fluoro (**27**) and 3-chloro (**29**) analogs all had AC_{50} values <800 nM. Notably, the 3-methoxy analog (**34**) saw a potency drop of >4-fold compared to the 3-methyl version. All *ortho*-substituents tested resulted in a marked decrease in activity while more tolerance

was observed at the *para*-position. Noteworthy inactive analogs were pyridine derivatives **31** and **32** as well as the quinoline derivative (**39**) for which the non-nitrogenous 2-naphthalene analog (**38**) had reasonable activity (1.3 μM). Tethering the hydrophobic dimethyl group in a dihydroindene ring resulted in a much less potent analog (**40**), while combinations of methyl, fluoro and chloro at the 3- and 4-positions resulted in a number of analogs with good potencies (**41** – **46**). Both the 3-chloro-4-methyl (**41**) and 3-chloro-4-fluoro (**45**) derivatives had potencies <300 nM, so these, along with the original 3,4-dimethyl substitution patterns were chosen as motifs to carry on.

Derivatives with various substituents at the 6-position of 3,4-dihydroquinolin-2(1H)-one-7-sulfonamides, the 7-position of 3,4-dihydroquinolin-2(1H)-one-6-sulfonamides, and the 6-position of 3-oxo-3,4-dihydro-2H-benzo[b][1,4]oxazine-7-sulfonamides were examined next (Table 3). 6-bromo-3-oxo-3,4-dihydro-2H-benzo[b][1,4]oxazine-7-sulfonyl chloride was coupled with 3,4-dimethylaniline and then subjected to standard Suzuki cross coupling conditions to provide a variety of aryl substituted dihydro-2H-benzo[b][1,4]oxazines (Scheme 2A). Generally, the addition of aryl and heteroaryl substituents resulted in decreased reactivity (exemplified by **47** and **48** in Table 3).

Good activity was obtained starting with 7-fluoro-2-oxo-1,2,3,4-tetrahydroquinoline-6-sulfonyl chloride to generate **51** with a potency of 210 nM. This particular analog was further modified by introduction of nitrogen nucleophiles through S_NAr reactions in acetonitrile (Scheme 2B). Significant SAR was seen with substitution of a variety of these analogs. Sterically larger groups like N,N-dimethylpyrrolidin-3-amine (**56**) and piperidine (**57**) resulted loss of activity while smaller dimethyl- (**52**) and methyl-amine (**54**) derivatives retained activity. With the realization that small amines were tolerated at this position a few analogs were generated in an effort to improve both solubility and potency (**58** – **63**). The racemic alaninol derivative provided high aqueous kinetic solubility (>120 μM in PBS buffer) while retaining low nanomolar potency (**61**). Preparation of the enantiopure versions with (*S*)- and (*R*)-alaninol resulted the (*S*)-derivative being 4-fold more potent than its enantiomer (880 nM for **62** vs 170 nM for **63**). Combination of 7-fluoro or 7-(*S*)-alaninol derivatives with the best aniline analogs from Table 2 gave compounds **64** – **70**, which all have low nanomolar activity with good maximum response. Interestingly, it was discovered that flipping the amide orientation to generate the 6-chloro- and 6-(dimethylamino)-3,4-dihydroquinolin-2(1H)-one-7-sulfonamide derivatives gave potent analogs **71** – **73**. These results led us to develop chemistry to quickly access these constitutional isomers (Scheme 3). The sulfonylation of **78** generated regioisomers that after coupling with **79** afforded **74a** and **74b** or with aniline **80** afforded **75a** and **75b**. Analogs **74a** and **75a** had weak activity (>5μM) while their regioisomers, **74b** and **75b** had no activity (data not shown). The incorporation of the (*S*)-alaninol through Ullmann chemistry for the active bromide isomers generated **76a** and **77a**, but rather surprisingly, these compounds had significantly diminished activity compared to analogs **63** and **68** respectively. Buchwald chemistry was required for the conversion of **74b** and **75b** to the alaninol-substituted derivatives **76b** and **77b**, respectively. Both of these analogs proved to be inactive, as well (data not shown).

Having generated a number of analogs with potencies <200 nM, a select few were taken on to assess their selectivity against the other PK isoforms (Figure 2). All analogs tested had no activity against the R or M1 isoforms and showed only minimal activation of the L isoform (≤25% at 57.5 μM). Compound **66** was also tested for its ability to modulate PEP and ADP affinity for hPKM2 (Figure 3). As with our previously reported activators [16,17], this analog showed significant decrease in K_m for PEP (K_m ~ 1.9 mM without **66**, 0.4 mM with **66**) while not affecting the K_m of ADP (K_m ~ 0.1 mM in both conditions). A number of analogs were also taken on to test their cell permeability and *in vitro* microsomal stability in both mouse and human liver microsomes (Caco-2, MLM and HLM in Table 4). While the

original lead (**3**) had moderate Caco-2 permeability with an efflux ratio <1, it had poor microsomal stability in both mouse and human liver microsomes ($t_{1/2}$<20 minutes). It became apparent that while the alaninol substituent provided good solubility and potency, high efflux ratios and reduced MLM half lives were attributable to the incorporation of this side-chain (**68** and **69** in Table 4). A more drastic reduction in microsomal stability was seen with the *N*-methyl- and *N*,*N*-dimethyl-derivatives **52** and **54** both having half lives <25 minutes. This data suggests that alkyl-amine substitution at this position engenders the molecules with efflux and/or microsomal stability liabilities. Compounds showing good permeability and efflux ratios (≤1) had either hydrogen or fluorine substituents at the 7-position (**3, 64** and **66**). The metabolic liabilities of the *meta*- and *para*-groups was assessed by comparing analogs **51**, **64** and **66.** Switching the *meta*-methyl group to a *meta*-chlorine slightly decreased both human and mouse microsomal stability (compare **64** to **51**). Further, switching the *para*-methyl group on **64** to a *para*-fluorine on **66** saw a marked increase in both HLM and MLM with a half life of 277.2 and 117.5 minutes respectively.

In conclusion, we have developed a third novel chemotype capable of activating PKM2. These molecules, based on the 2-oxo-*N*-aryl-1,2,3,4-tetrahydroquinoline-6-sulfonamide scaffold, have low nanomolar potency with a notable analog, **66**, having an AC_{50} of 90 nM with selectivity over other PK isoforms, good Caco-2 permeability, a low efflux ratio (0.84) and high microsomal stability ($t_{1/2}$ = 277.2 min in HLM and 117.5 min in MLM).

Acknowledgments

We thank Paul Shinn, Danielle VanLeer and Christopher LeClair for assistance with compound management. This research was supported by the Molecular Libraries Initiative of the NIH Roadmap for Medical Research and the Intramural Research Program of the National Human Genome Research Institute, National Institutes of Health.

References

1. Mazurek S, Boschek CB, Hugo F, Eigenbrodt E. Semin Cancer Biol. 2005; 15:300–308. [PubMed: 15908230]
2. Reinacher M, Eigenbrodt E. Virchows Arch B Cell Pathol Incl Mol Pathol. 1981; 37:79–88. [PubMed: 6116351]
3. Christofk HR, Vander Heiden MG, Harris MH, Ramanathan A, Gerszten RE, Wei R, Fleming MD, Schreiber SL, Cantley LC. Nature. 2008; 452:230–233. [PubMed: 18337823]
4. Christofk HR, Vander Heiden MG, Wu N, Asara JM, Cantley LC. Nature. 2008; 452:181–186. [PubMed: 18337815]
5. Vander Heiden MG, Locasale JW, Swanson KD, Sharfi H, Heffron GJ, Amador-Noguez D, Christofk HR, Wagner G, Rabinowitz JD, Asara JM, Cantley LC. Science. 2010; 329:1492–1499. [PubMed: 20847263]
6. Levine AJ, Puzio-Kuter AM. Science. 2010; 330:1340–1344. [PubMed: 21127244]
7. Vander Heiden MG, Cantley LC, Thompson CB. Science. 2009; 324:1029–1033. [PubMed: 19460998]
8. Luo W, Hu H, Chang R, Zhong J, Knabel M, O'Meally R, Cole RN, Pandey A, Semenza GL. Cell. 2011; 145:732–744. [PubMed: 21620138]
9. Kenzaburo T, Yoshida MC, Hitoshi S, Keiji M, Tamio N, Takehiko T, Hisaichi F, Shiro M. Gene. 1988; 73:509–516. [PubMed: 2854097]
10. Satoh H, Tani K, Yoshida MC, Sasaki M, Miwa S, Fujii H. Cytogenet Cell Genet. 1988; 47:132–133. [PubMed: 3378452]
11. Takenaka M, Yamada K, Lu T, Kang R, Tanaka T, Noguchi T. Eur J Biochem. 1996; 235:366–371. [PubMed: 8631356]
12. Noguchi T, Inoue H, Tanaka T. J Biol Chem. 1986; 261:13807–13812. [PubMed: 3020052]
13. Noguchi T, Yamada K, Inoue H, Matsuda T, Tanaka T. J Biol Chem. 1987; 262:14366–14371. [PubMed: 3654663]

14. Dombrauckas JD, Santarsiero BD, Mesecar AD. Biochemistry. 2005; 44:9417–9429. [PubMed: 15996096]

15. Mazurek S. Int J Biochem Cell Bio. 2011; 43:969–980. [PubMed: 20156581]

16. Boxer MB, Jiang JK, Vander Heiden MG, Shen M, Skoumbourdis AP, Southall N, Veith H, Leister W, Austin CP, Park HW, Inglese J, Cantley LC, Auld DS, Thomas CJ. J Med Chem. 2010; 53:1048–1055. [PubMed: 20017496]

17. Jiang JK, Boxer MB, Vander Heiden MG, Shen M, Skoumbourdis AP, Southall N, Veith H, Leister W, Austin CP, Park HW, Inglese J, Cantley LC, Auld DS, Thomas CJ. Bioorg Med Chem Lett. 2010; 20:3387–3393. [PubMed: 20451379]

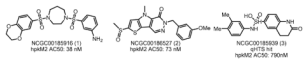

Figure 1.
Chemical Structures of Previously Reported hPKM2 Activators NCGC00185916 (**1**), NCGC00186527 (**2**) and qHTS Hit NCGC00185939 (**3**).

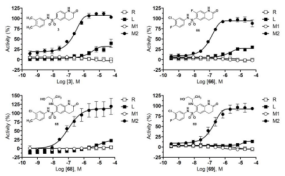

Figure 2.
Pyruvate Kinase Isoform Selectivity Profile.

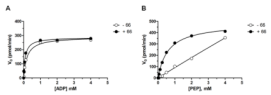

Figure 3.

Compound **66** affects PEP affinity, but not ADP affinity. (A) Initial velocity as a function of ADP concentration in the absence (○) or presence (●) of **66** (10 μM). (B) Initial velocity as a function PEP concentration in the absence (○) or presence (●) of **66** (10 μM). Vo, initial rate in pmol/min as determined in the PK-LDH coupled assay (kinetic assays were carried out at approximately 22 °C with 10 nM PKM2 using [KCl] = 200 mM, [$MgCl_2$] = 15 mM, and with either [ADP] or [PEP] = 4.0 mM; see Supporting Information).

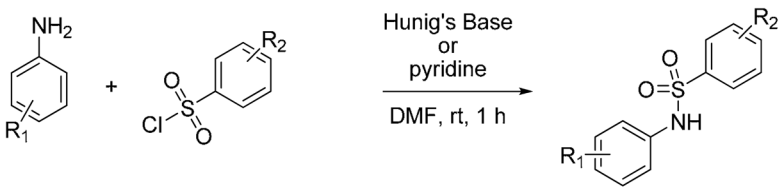

Scheme 1.
General Synthetic Methodology Used to Access Analogs in Tables 1 and 2.

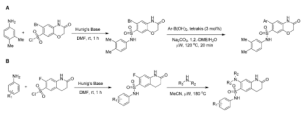

Scheme 2.
General Synthetic Methodology Used to Access Analogs in Table 3.

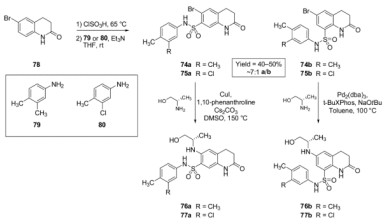

Scheme 3.
Synthesis of 6-Substituted 3,4-Dihydroquinolin-2(1H)-one-7-sulfonamides

Table 1

SAR of N-(3,4-Dimethylphenyl)arylsulfonamides

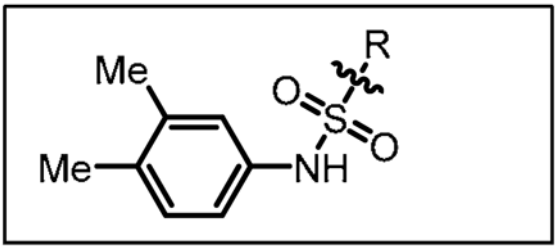

#	R	hPK M2 AC_{50} (μM)[a]	hPK M2 max resp. (%)[b]
4	5-(*N*-methylindole)	19.9	47
5	3-(benzoic acid)	>20	NA
6	4-fluoro-C_6H_4	>20	NA
7	2-napthalene	18.4	69
8	3-chloro-C_6H_4	18.3	71
9	4-methoxy-C_6H_4	17.3	53
10	6-(2,2-dimethylchroman)	10.0	62
11	6-(2*H*-benzo[*b*][1,4]oxazin-3(4*H*)-one)	13.4	81
12	5-(1*H*-benzo[*d*]imidazol-2(3*H*)-one)	>20	NA
13	3-*N*HAcetyl-C_6H_4	13.1	58
14	6-(*N*-acetyl-tetrahydroquinoline)	9.0	76
15	5-(indolin-2-one)	8.3	57
16	7-(4,5-dihydro-1*H*-benzo[*b*]azepin-2(3*H*)-one)	7.1	88
17	4-*N*HAcetyl-C_6H_4	6.9	<40
18	6-(3-methylbenzo[*d*]oxazol-2(3*H*)-one)	4.3	95
19	6-(4-methyl-3,4-dihydro-2*H*-benzo[*b*][1,4]oxazine)	6.0	81
20	4-(2-oxopyrrolidin-1-yl)-C_6H_4	0.94	60
21	5-(1-methylindolin-2-one)	2.3	119
22	5-(N-acetyllindoline)	1.5	96

[a] AC_{50} values were determined utilizing the luminescent pyruvate kinase-luciferase coupled assay (ref. 16) and the data represents the average from three separate experiments. Max Res. (Maximum Response) is % activity that represents the % activation at 57 μM of compound. See supporting information for normalization.

Table 2

SAR of 2-Oxo-1,2,3,4-tetrahydroquinoline-6-sulfonamides

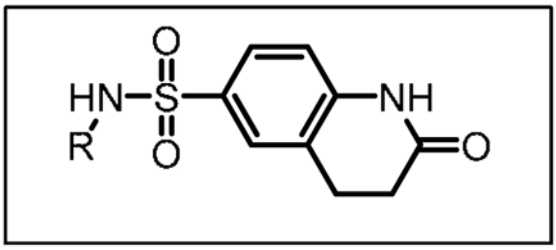

#	R	hPK M2 AC_{50} (μM)[a]	hPK M2 Max Resp. (%)[b]
23	2-methyl-benzene	2.2	94
24	3-methyl-benzene	0.25	101
25	4-methyl-benzene	1.4	102
26	2-fluoro-benzene	5.2	95
27	3-fluoro-benzene	0.79	101
28	4-fluoro-benzene	6.0	84
29	3-chloro-benzene	0.41	104
30	4-chloro-benzene	2.0	106
31	4-(pyridine)	>20	NA
32	3-(pyridine)	>20	NA
33	4-methoxy-benzene	16.3	85
34	3-methoxy-benzene	1.1	115
35	3-phenyl-benzene	>20	NA
36	6-(2,3-dihydrobenzo[*b*][1,4]dioxine)	11.1	100
37	3-trifluoromethyl-benzene	6.4	109
38	2-napthalene	1.3	121
39	6-(quinoline)	>20	NA
40	5-(2,3-dihydro-1*H*-indene)	4.6	73
41	3-chloro-4-methyl-benzene	0.10	104
42	3,4-dichloro-benzene	1.3	95
43	4-chloro-3-methyl-benzene	0.56	121
44	3-fluoro-4-methylbenzene	0.54	138
45	3-chloro-4-fluoro-benzene	0.29	123
46	4-fluoro-3-methyl-benzene	0.44	128

[a] AC_{50} values were determined utilizing the luminescent pyruvate kinase-luciferase coupled assay (ref. 16) and the data represents the average from three separate experiments. Max Res. (Maximum Response) is % activity that represents the % activation at 57 μM of compound. See supporting information for normalization.

Table 3

SAR of 3,4-Dihydroquinolin-2(1H)-one-7-sulfonamides, 3,4-Dihydroquinolin-2(1H)-one-6-sulfonamides and 3-Oxo-3,4-dihydro-2H-benzo[b][1,4]oxazine-7-sulfonamides

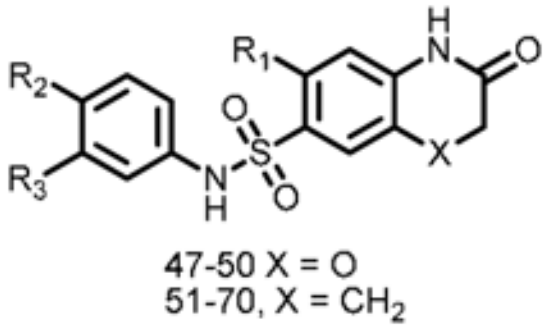

#	R_1	R_2	R_3	hPK M2 AC_{50} (μM)[a]	hPK M2 Max Resp. (%)[b]
47	phenyl	Me	Me	>20	NA
48		Me	Me	>20	NA
49	methyl	Me	Me	0.48	111
50	CI	Me	Me	0.26	80
51	F	Me	Me	0.21	101
52		Me	Me	0.22	129

#	R_1	R_2	R_3	hPK M2 AC_{50} (μM)[a]	hPK M2 Max Resp. (%)[b]
53		Me	Me	3.8	106
54		Me	Me	0.44	102
55		Me	Me	0.51	123

#	R_1	R_2	R_3	hPK M2 AC_{50} (μM)[a]	hPK M2 Max Resp. (%)[b]
56	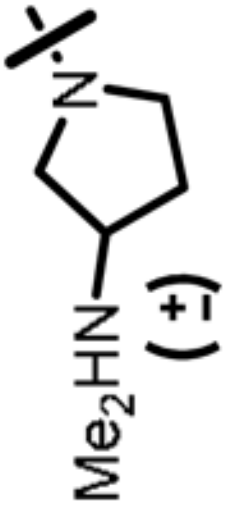	Me	Me	>20	NA
57		Me	Me	18.3	47
58	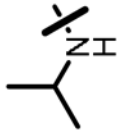	Me	Me	0.57	123

#	R_1	R_2	R_3	hPK M2 AC_{50} (μM)[a]	hPK M2 Max Resp. (%)[b]
59	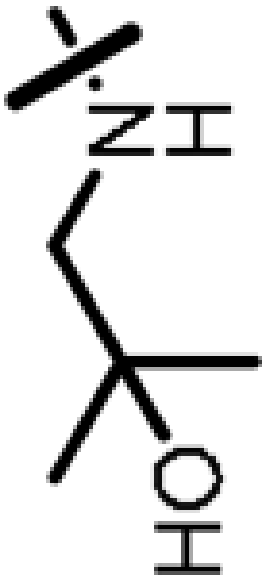	Me	Me	2.1	83
60		Me	Me	0.18	132
61	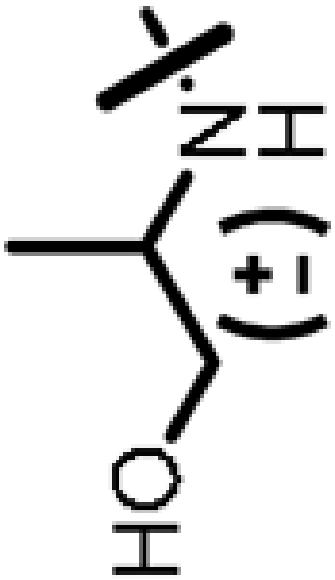	Me	Me	0.23	124

#	R_1	R_2	R_3	hPKM2 AC_{50} (μM)[a]	hPKM2 Max Resp. (%)[b]
62	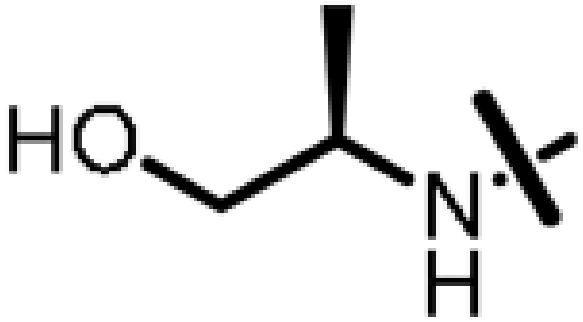	Me	Me	0.88	108
63	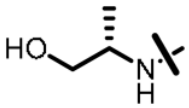	Me	Me	0.17	116
64	F	Me	CI	0.14	112
65	F	CI	Me	0.60	93
66	F	F	CI	0.09	88
67	F	F	Me	0.24	92
68	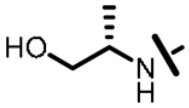	Me	CI	.06	96
69	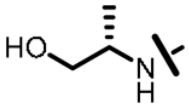	F	CI	0.13	92

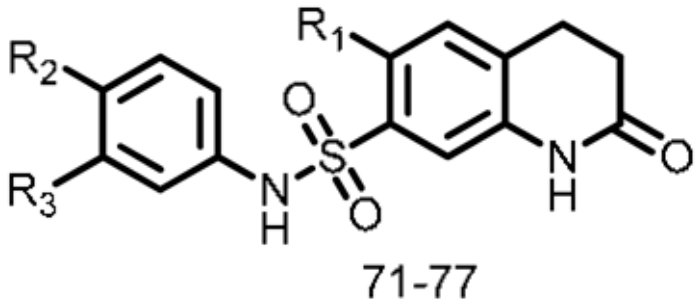

71-77

#	R_1	R_2	R_3	hPKM2 AC_{50} (μM)[a]	hPKM2 Max Resp. (%)[b]
70	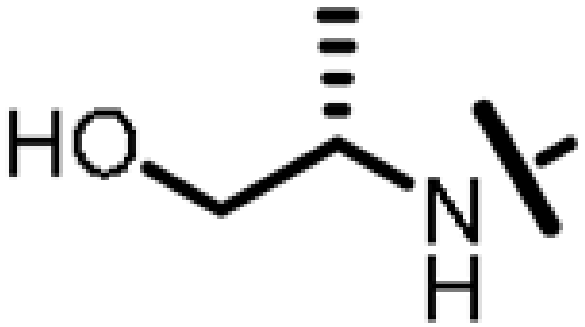	F	Me	0.29	95
71	CI	Me	Me	0.07	92
72	CI	Me	CI	0.09	109
73	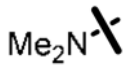	Me	Me	0.21	106
74a	Bra	Me	Me	6.60	52
75a	Bra	Me	CI	7.43	51
76a	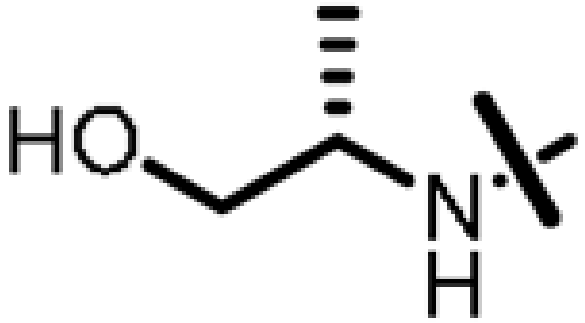	Me	Me	6.1	66

#	R_1	R_2	R_3	hPKM2 AC_{50} (μM)[a]	hPKM2 Max Resp. (%)[b]
77a	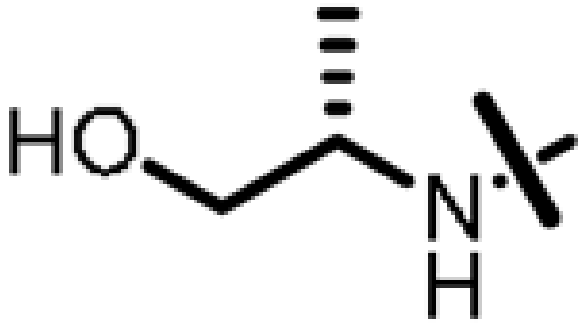	Me	Cl	6.1	54

[a] AC_{50} values were determined utilizing the luminescent pyruvate kinase-luciferase coupled assay (ref. 16) and the data represents the average from three separate experiments. Max Res. (Maximum Response) is % activity that represents the % activation at 57 μM of compound. See supporting information for normalization.

Table 4

Microsomal Stability and Caco-2 Permeability of Select Compounds

	In vitro Microsomal Stability[a] $t_{1/2}$ (min)		Caco-2 Permeability[a]		
Compound	**HLM**	**MLM**	**$P_{app\ (A–B)}$ (10^{-6}, cm/s)**	**$P_{app\ (B–A)}$ (10^{-6}, cm/s)**	**Efflux Ratio**
3	6.0	17.3	14.9	12.21	0.82
64	22.9	54.1	6.22	6.24	1
66	277.2	117.5	9.38	7.91	0.84
69	78.8	36.3	1.61	17.52	10.91
68	30.4	22.9	1.13	11.9	10.51
52	19.4	21.7	ND	ND	ND
51	16.5	34.3	ND	ND	ND
54	19.7	19.1	ND	ND	ND

[a] See supporting information for experimental procedures

Bioorg Med Chem Lett. Author manuscript; available in PMC 2011 December 1.